Beyond the percolation universality class: the vertex split model for tetravalent lattices



2015 New J. Phys. 17 043061

(http://iopscience.iop.org/1367-2630/17/4/043061)

New Journal of Physics
The open access journal at the forefront of physics

Deutsche Physikalische Gesellschaft DPG
IOP Institute of Physics

Published in partnership with: Deutsche Physikalische Gesellschaft and the Institute of Physics

OPEN ACCESS

RECEIVED
8 December 2014

REVISED
19 March 2015

ACCEPTED FOR PUBLICATION
27 March 2015

PUBLISHED
29 April 2015



PAPER

# Beyond the percolation universality class: the vertex split model for tetravalent lattices

**Susan Nachtrab**[1], **Matthias J F Hoffmann**[1], **Sebastian C Kapfer**[1], **Gerd E Schröder-Turk**[1,2] **and Klaus Mecke**[1]

[1] Institut für Theoretische Physik, Friedrich-Alexander Universität Erlangen-Nürnberg, Staudtstr. 7, D-91058 Erlangen, Germany
[2] School of Engineering & Information Technology, Mathematics & Statistics, Murdoch University, 90 South St, Murdoch, WA 6150, Australia

**E-mail:** g.schroeder-turk@murdoch.edu.au **and** klaus.mecke@fau.de

**Keywords:** percolation, networks in phase transitions, mechanical properties of solids

## Abstract

We propose a statistical model defined on tetravalent three-dimensional lattices in general and the three-dimensional diamond network in particular where the splitting of randomly selected nodes leads to a spatially disordered network, with decreasing degree of connectivity. The terminal state, that is reached when all nodes have been split, is a dense configuration of self-avoiding walks on the diamond network. Starting from the crystallographic diamond network, each of the four-coordinated nodes is replaced with probability $p$ by a pair of two edges, each connecting a pair of the adjacent vertices. For all values $0 \leqslant p \leqslant 1$ the network percolates, yet the fraction $f_p$ of the system that belongs to a percolating cluster drops sharply at $p_c = 1$ to a finite value $f_p^c$. This transition is reminiscent of a percolation transition yet with distinct differences to standard percolation behaviour, including a finite mass $f_p^c > 0$ of the percolating clusters at the critical point. Application of finite size scaling approach for standard percolation yields scaling exponents for $p \to p_c$ that are different from the critical exponents of the second-order phase transition of standard percolation models. This transition significantly affects the mechanical properties of linear-elastic realizations (e.g. as custom-fabricated models for artificial bone scaffolds), obtained by replacing edges with solid circular struts to give an effective density $\phi$. Finite element methods demonstrate that, as a low-density cellular structure, the bulk modulus $K$ shows a cross-over from a compression-dominated behaviour, $K(\phi) \propto \phi^{\kappa}$ with $\kappa \approx 1$, at $p = 0$ to a bending-dominated behaviour with $\kappa \approx 2$ at $p = 1$.

*Percolation* is a fundamental model of statistical physics and probability theory [1], with a wealth of scientific and engineering applications [2]. The fundamental question of percolation theory is the existence of connected components whose size is of the order of the system size (*percolating clusters*), in disordered structures that result from randomly inserting or removing local structural elements. It owes its generality, and hence importance, partially to the strong universality of the percolation transition. In the majority of lattice and continuum models, the transition from non-percolating to percolating structures is a continuous second-order phase transition in the insertion (or deletion) probability $p$, characterized by the same critical exponents that are independent of lattice type, symmetry, coordination, particle shape, etc [1]. Exceptions are non-equilibrium directed percolation models [3, 4] and negative-weight percolation [5], both with different critical exponents, and explosive percolation where a bias for the formation of small clusters leads to a first order transition [6, 7] or at least to unusual finite size scaling [8].

We propose a simple statistical model, here referred to as *vertex split model* or *linked loop model*, defined for the three-dimensional diamond network. (The diamond network is the crystallographic net with cubic symmetry $Fd\bar{3}m$ consisting of a single type of edge and vertex. Four edges meet at every vertex, forming tetrahedral angles [9].) Rather than deleting spatial elements from the diamond network, such as bonds or vertices, the random operation consists of reducing the vertex coordination by replacing, with probability $p$, each four-coordinated vertices with pairs of two-coordinated vertices, see figures 1 and 2. This induces a

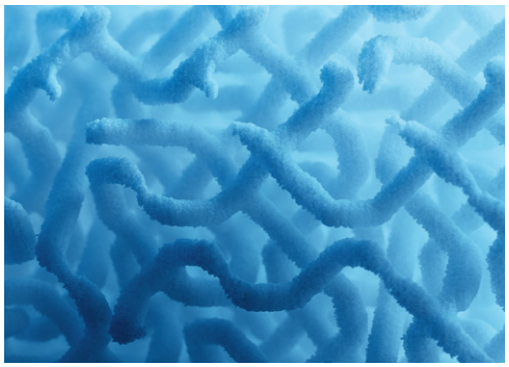

**Figure 1.** Realization of a vertex split model based on the Diamond lattice, custom-fabricated by 3D printing of ABS plastic. In the context of bone scaffold engineering, vertex splitting has been suggested [10] as an efficient way of adjusting stiffness as a key mechanical property.

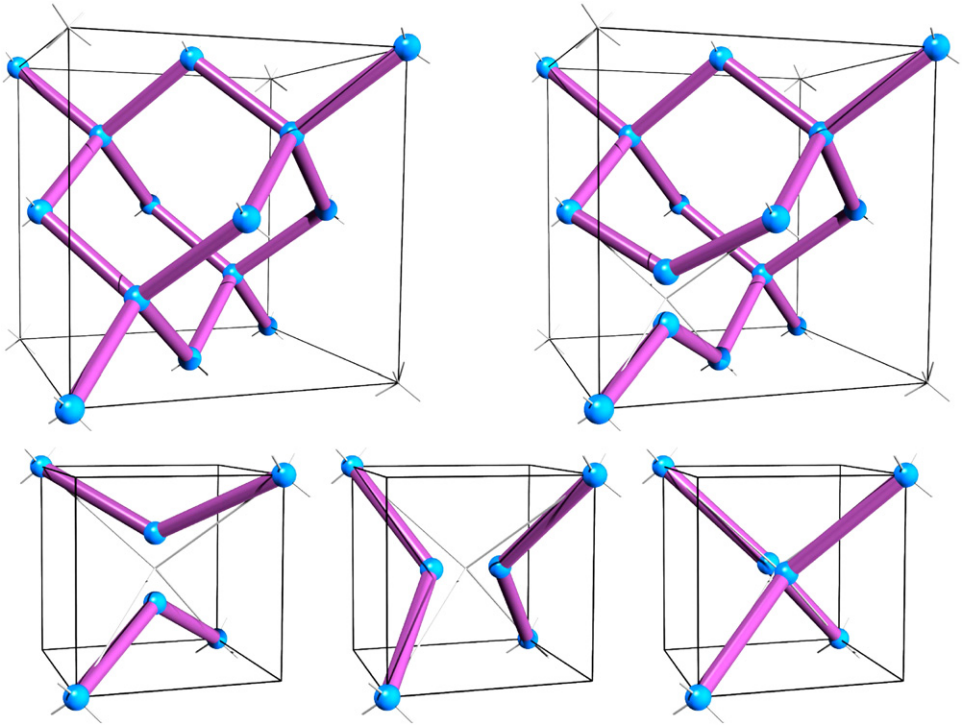

**Figure 2.** A unit cell of the crystallographic diamond network with four-coordinated nodes (top, left) and the network that results from severing one of the nodes (top, right). Each node remains unchanged with probability $(1 - p)$, or is severed (or split) into two pairs of edges, with the three possible configurations for neighbour pairs selected with equal probability $p/3$ (bottom).

transition from a fully coordinated crystalline network at $p = 0$ to a network filled densely with self-avoiding random walks. The two names are motivated by two different perspectives; with reference to the ordered fully-connected crystalline diamond network at $p = 0$, *vertex splitting* is the operation that leads to the transition studied here. From the alternative perspective of the state at $p = 1$, represented by a dense set of self-avoiding walks, the model may be defined as the random insertion of 'links' between adjacent, infinite or finite loops with probability $(1 - p)$.

Each unsevered vertex of the diamond network has four edges connecting the vertex to four distinct neighbour vertices. Each vertex of the diamond network is split (or severed) with probability $p$, that is, the four-coordinated node is replaced by two two-coordinated nodes slightly displaced from the position of the original four-coordinated node, see figure 2. When splitting a node, the three possible configurations for neighbour pairs are selected with equal probability. Note that the parameter $p$ is the probability to *degrade* a four-link, opposite to the conventional use of $p$ in bond/site percolation models as the probability to *create* a bond or site.

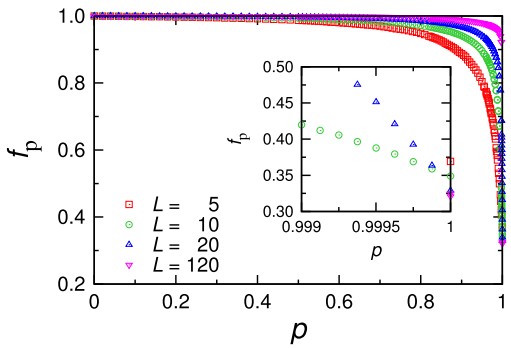


**Figure 3.** Fraction $f_p$ of edges belonging to any of the percolating clusters. The insert is a close-up, demonstrating a finite value $f_p^c$ of $f_p$ at $p_c = 1$. All data in figures 3–10 is obtained with lateral periodic boundary conditions.

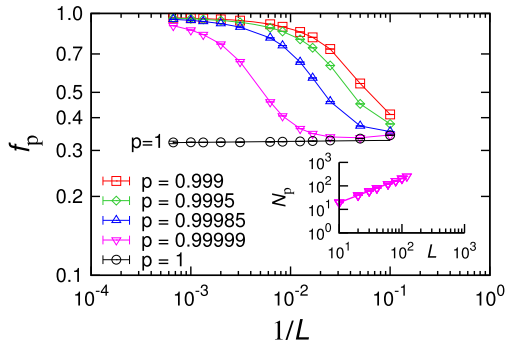


**Figure 4.** Dependence of $f_p$ on the linear system size $L$, for fixed $p$. ($8 \times L^3$ is the number of vertices.) The insert shows the number $N_p$ of percolating clusters as function of $L$. Note that, at $p = p_c$, the difference $[f_p^c(L) - f_p^c(L = \infty)]$ to the finite value at $p_c$ (rather than the absolute value $f_p^c(L)$) is commensurate with the functional form $[f_p^c(L) - f_p^c(L = \infty)] \propto L^{-0.9}$, representing the small deviations from a constant behaviour for small system sizes.

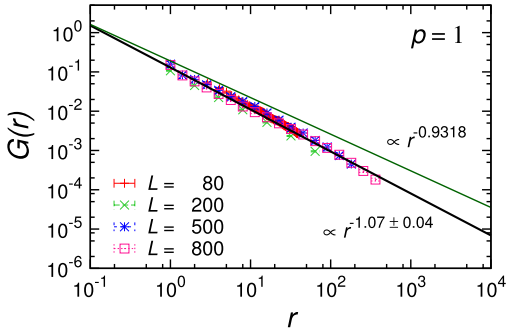


**Figure 5.** The averaged pair-connectedness function $G(r)$, for $p = p_c$, for different linear system size $L$. The decay follows a power law with exponent $(d - 2 - \eta) = -1.07 \pm 0.04$, significantly different from the site percolation value −0.9318.

Connected components define clusters, the size of which is measured by the number of constituent edges. A cluster is considered *percolating* if it traverses the system in $z$-direction from top to bottom[3]. Systems with both periodic and open boundary conditions in the lateral $x$ and $y$ directions are considered, but all data in figures 3–10 are for periodic boundary conditions (a further possibility represented by a fully periodic system

[3] Note however that the network itself has cubic symmetry and the severing process induces no anisotropy. In fact, in terms of the effective linear-elastic properties, the system becomes more isotropic with increasing $p$, such that the difference between the two shear moduli (in a system with initially cubic symmetry) vanishes for large $p$, see insert in figure 3(B) in [10]. This mechanical isotropy relates presumably also to higher structural isotropy, in a statistical sense.

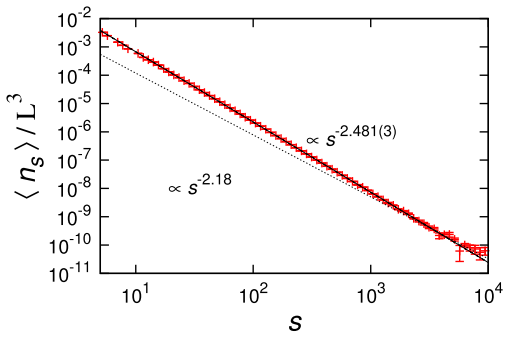


**Figure 6.** Power law decay $\langle n_s \rangle \propto s^{-\tau}$ at transition $p = p_c$ of the vertex split model. Contrary to standard bond or site percolation a finite size scaling is necessary to find the correct scaling behaviour. $n_s$ is the number of clusters of size $s$ obtained from the finite size scaling via $n_s(L) = n_s + t_0\, L^{-\nu}$. The exponent $\tau \approx 2.481 \pm 0.003$ is greater than 2 and hence decays sufficiently fast for $\sum_{s=0}^{\infty} s n_s$ to converge to a finite value, but it is different from the value for the site percolation exponent $\tau \approx 2.19$ [11].

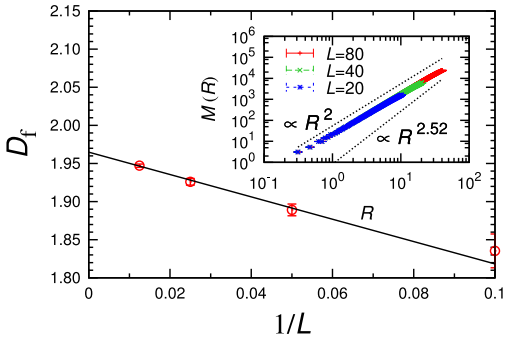


**Figure 7.** The fractal dimension of the percolating cluster at $p = p_c$ is estimated as $D_f = 1.97 \pm 0.06$. This estimate is obtained by fitting a straight line $a\ R + b$ to the values of average mass of the percolating clusters $M(R)$, see insert for a given system size $L$. The fractal dimension is obtained by fitting a straight line to the values of $a$ as function of $1/L$. Data in the insert is averaged over 100 or more realizations. The error estimate for $D_f$ corresponds to the variations observed for different system sizes $L = 10,\ 20,\ 40,\ 80$ ($L = 10$ not shown).

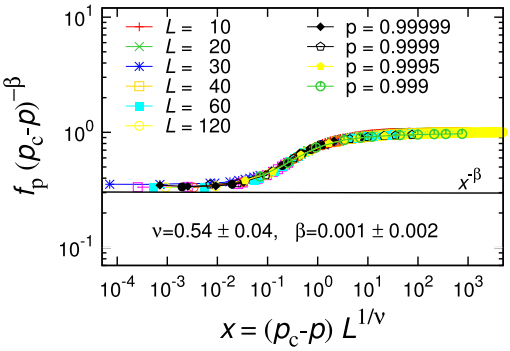


**Figure 8.** Extraction of $\beta$ and $\nu$ from finite size scaling of $f_p$: the scaling function is expected to become constant for $x = (p - p_c)L^{1/\nu} \gg 1$, and to decrease as $x^{-\beta}$ for $x \ll 1$. Error margins represent the half-width of the intervals for $\beta$ and $\nu$ for which the scaling behaviour is similarly close as for the estimated best values $\nu = 0.54$ and $\beta = 0.001$.This plot assumes validity of the conventional finite size scaling for $f_p(L)$ rather than $f_p(L) - f_p^c$, an assumption that is complicated by the finite value of $f_p$ at $p = p_c$ and by the fact that there is no non-percolating phase.

was not investigated here); system size is measured in the number $L^3$ of unit cells, each comprising eight vertices of the network, see figure 2.

Figure 3 shows the fraction of percolating edges $f_p$ as function of $p$, for different system sizes $L$, suggesting a transition at $p_c = 1$. Over the entire interval $p \in [0,\ 1]$ we find the system to represent percolating configurations. However, $p_c = 1$ represents a critical point where the fraction $f_p$ of edges belonging to percolating

**Table 1.** Thresholds and exponents of the vertex split model and of the site percolation model, both on the diamond network. The critical exponents for the site percolation model are values from [1, 11, 12], with the percolation threshold for the diamond network reproduced from [13]. For $\beta$ and $\nu$ we have verified that our implementation of the site percolation model reproduces these results. Note that we have not been able to obtain consistent estimates for the exponent $\nu$ prescribing the decay of the correlation lengths, for the vertex split model. The two estimates based on finite size scaling of quantities at $p = p_c$ yield values around 1.0 whereas the estimate based on finite size scaling of quantities at $p < 1$ yields $\nu = 0.54$, differing by a factor of very close to 2. We speculate that this discrepancy is likely due to the multiplicity of the percolating cluster at $p = p_c$, or to the possibility that the transition is not of second order. Note the discussion relating to $\beta$ in item (iii) in the main text. For the scaling exponents of the vertex split model, error bars combine variances of the data (statistical error of fit) with variations when changing fitting ranges and system size. All data is for periodic boundary conditions in the lateral directions; see [14] for data for open boundary conditions.

| | Site | Vertex split | Figure |
|---|---|---|---|
| Threshold | $p_c = 0.569$ | 1 | 3 and 4 |
| Edges in infinite cluster(s) | | | |
| $f_p \sim (p - p_c)^\beta$ | $\beta = 0.41$ | $0.001 \pm 0.002$ | 8 and 4 |
| Correlation length | | | |
| $\xi \sim \lvert p - p_c \rvert^\nu$ | $\nu = 0.88$ | $0.54 \pm 0.04$ | 4 |
| | | $\approx 1.0$ | 6 |
| Pair-connectedness function | | | |
| $G(r) \sim r^{-(d-2+\eta)}$ | $\eta = -0.068$ | $0.07 \pm 0.04$ | 5 |
| Cluster size distribution | | | |
| $\langle n_s \rangle \sim s^{-\tau}$ | $\tau = 2.189$ | $2.481 \pm 0.003$ | 6 |
| Fractal dimension | | | |
| | $D_f = 2.52$ | $1.97 \pm 0.06$ | 7 |

clusters sharply drops, to a value $f_p^c > 0$ which is finite; the model has no non-percolating phase. $f_p$ is defined as the ratio $s_p/S$ of the number of all edges that belong to percolating clusters, $s_p := \sum_{j \in \mathcal{P}} s(j)$, where $\mathcal{P}$ is the set of all percolating clusters and $s(j)$ the number of edges in cluster $j$, to the total number $S$ of edges in the system.

Figure 4 shows $f_p$ as function of system size $L$, for various $p$ near $p_c$ and for periodic boundary conditions. This demonstrates that for $p < p_c = 1$ the percolating fraction $f_p$ of the system increases with $L$; for large systems and $p < 1$ a vast majority of the edges belong to percolating clusters. By contrast, at $p = p_c = 1$, $f_p$ varies only very slightly with $L$, despite our analysis including very large systems with up to $2.7 \times 10^{10}$ vertices. Linear regression yields a slope of $f_p(1/L)$ of value $0.002 \pm 0.002$, which our analysis cannot distinguish from a constant behaviour, $f_p(L) = \text{const}$ (the error margin combines the statistical variance of the data around their mean and systematic variations observed when varying the fit interval). When formally interpreting this in the framework of standard finite size scaling for the second-order percolation transition, this leads to an interpretation of this slope as $\beta/\nu = 0.002 \pm 0.002 \approx 0$ for the power-law $f_p \propto L^{-\beta/\nu}$, for $p \neq p_c$ and bearing in mind the discontinuity at $p_c$. This analysis is further support of our claim of a transition at $p_c = 1$. The data for open boundary conditions in the lateral directions (shown in [14]) are qualitatively similar, yet with the absolute values of $f_p^c$ approximately a factor of 10 smaller. Note in particular that this behaviour implies that the mass of the percolating cluster(s) is a finite value $f_p(p_c) = f_p^c > 0$, even for infinitely large systems $L \to \infty$, in contrast to the standard percolation models.

The insert of figure 4 shows the number of percolating clusters at $p = p_c = 1$ as a function of system size $L$. Importantly, in contrast to bond or site percolation, the number of percolating clusters at $p_c$ is not 1, but grows (within the limits of our numerical resolution) linearly with system size, $N_p \propto L$. The three possible types of unbranched self-avoiding paths for systems with lateral periodic boundary conditions are closed loops, percolating clusters (traversing the system in $z$-direction) and *u-turns*, i.e. clusters that return to the same end (bottom or top) of the network from where they emanated. The probability that a cluster emanating from one of the $4L^2$ sites at $z = 0$ percolates appears to be inversely proportional to the system height, $\propto 1/L$. As any $u$-turn cluster occupies two sites at $z = 0$, $N_p$ must be even or zero.

Figures 4–8 support the claim that the transition at $p_c = 1$ is a phase transition with scaling behaviour given by power-law decay for the characteristic quantities listed in table 1. The scaling exponents are significantly different from the critical exponents of conventional bond or site percolation, substantiating

the claim that the transition of the vertex split model is different from the universality class of standard percolation.

We comment on some aspects of the numerical extraction of these exponents from the numerical data. First, the observation that for $p = p_c$, $f_p(L) = \text{const}$ shows no statistically significant dependence on $L$ is possible without having to resort to finite size scaling (figure 4); even for small systems, such as $L = 100$, we observe only small differences in $f_p$ from the value for large systems, at $p = p_c = 1$. Note however the complication that $f_p$ does not drop to 0 but to a finite value $f_p^c > 0$ at $p_c$ and that a non-percolating phase (characterized by $f_p = 0$) does not exist; this raises the question if the appropriate order parameter is $f_p(L)$ or the difference $f_p(L) - f_p^c(L = \infty)$.

Second, the exponent $\tau$, describing the decay of the cluster size distribution $\langle n_s \rangle(s)$ at $p = p_c$ is substantially harder to determine, requiring the use of finite size scaling, despite large system sizes. The data in figure 6, is determined by using finite size scaling for $n_s$: the system-size independent value $n_s$ is extracted from the simulation data $n_s(L)$ for a system of size $L$ by $n_s(L) = n_s + t_0\, L^{-1/\nu}$, with a best fit obtained for $\nu = 1.0 \pm 0.1$. System sizes up to $L = 1000$ were simulated for this plot. An additional complication for the determination of $\tau$ is the presence of percolating clusters at $p = p_c$. For the bond/site percolation problem, there are no infinite percolating clusters in an infinite systems right at the critical point $p = p_c$. Assuming $f_p(L) = \text{const}$ at $p = p_c$, this is not the case in the model studied here. Therefore, the question of how to treat percolating clusters is in principle important for the determination of $\tau$. However, we find that for systems with the periodic boundary conditions described here, after the described finite size scaling the value of $\tau$ is the same regardless of whether one takes percolating clusters into account for $\langle n_s(L) \rangle$ or not. (We note that we have not been able to determine a consistent value of $\tau$ from systems with open boundary conditions; for that case, the determination is complicated by a cross-over behaviour.)

Several aspects of the model deserve further scrutiny.

(i) The scaling exponents of the vertex split model do not fulfil the scaling relations $d - D_f = \frac{\beta}{\nu}$ and $d - 2 + \eta = \frac{2\beta}{\nu}$, valid for bond or site percolation; their derivation assumes a single unique percolating cluster, in contrast to the many line-like percolating clusters in this model. Similarly, this may be the cause for the different estimates for $\nu$ from finite size scaling involving (a) only properties at $p = p_c$ and (b) properties also at $p < p_c$, see table 1.

(ii) The corresponding planar model of severing four-coordinated vertices of planar square lattices is closely related to hull percolation or hull exponents of standard percolation clusters [15–18], also with different critical behaviour from standard percolation; the relationship between the planar and the spatial case requires further exploration.

(iii) The system-size dependence of the fraction $f_p(L)$ of the system that belongs to percolating clusters warrants further exploration. The $L$-independence of $f_p$ for $p = p_c$ and the $L$-dependent behaviour for $p < p_c$ are commensurate with $\beta = 0$, within the quality of the data and within the framework of finite size scaling for second-order phase transitions. This implies that $f_p(p) \propto (p - p_c)^\beta$ is independent of $p$, for $p \neq p_c$. This is also commensurate with the data, and for $L \to \infty$ implies $f_p(p) = 1$ for $p < p_c$ with a sharp jump to a finite $f_p(p_c) < 1$ at $p_c$. The sharpness of the change at $p_c$ and the finite value of $f_p$ at $p_c$ also allude to the possibility that the transition is a first-order transition or that the difference $f_p(p) - f_p(p_c)$ is the parameter whose scaling behaviour should be studied.

(iv) The scaling properties—in particular the $L$-independence of $f_p$ at $p_c$—point to the possibility of an effective description of the system. The perspective of the 'loop link' model affords the interpretation that, at $p = 1$, the insertion of random links between adjacent pairs of self-avoiding random walks corresponds to a long-range effect, which induces the sharp (possibly first order) transition described above. This, as well as the link to Flory-type arguments for the scaling behaviour of polymer systems, requires further investigation, by models that effectively tune the characteristics of the self-consistent random walk configuration.

(v) The relationship between the state at $p = 1$ and random walk configurations deserve further investigation. Evidently, the configuration at $p = 1$ represents an assembly of random walks subject to a non-overlap condition. However, the value of the fractal dimension very close to 2 (which is the value expected for a random walk) suggests a relation of the system to random walks without the non-overlap constraint. Note further that the value of $D_f$ is close to 2 which is consistent with the value one obtains from the following argument. Given that $1/L$ percolating clusters emerge from the top and bottom boundaries and that the fraction of lattice sites belonging to percolating clusters does not depend on $L$, the size per percolating cluster is $\mathcal{O}(L^2)$ in line with the estimate of $D_f$.

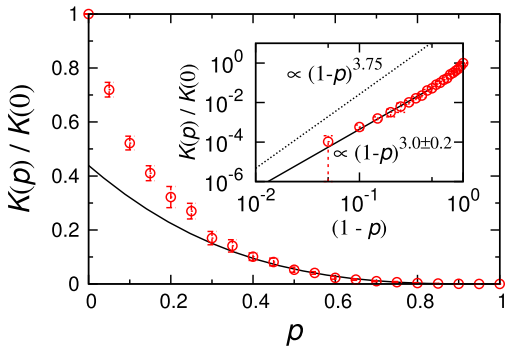


**Figure 9.** Bulk modulus $K(p)$ as a function of $p$ for the network solids obtained by dilating edges to cylinders, with solid volume fraction $\phi = 0.1$. The only relevant microscopic linear-elastic material constant is chosen as the Poisson's ratio $\nu_m = 0.5$. Data is computed for network solids of $4^3$ unit cells (512 vertices), discretized by $200^3$ voxels and averaged over five independent realizations. The insert shows that, near $p_c = 1$, the data follows a power-law with exponent ≈3.0 (determined by straight-line fitting to all data for $p \in [0.1,\ 0.5]$), different from the site percolation value $f_c = 3.75$ [12].

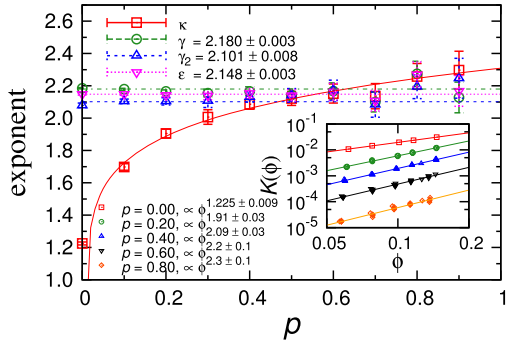


**Figure 10.** For fixed $p$, the effective bulk modulus $K$ and the shear moduli $G_1$ and $G_2$ obey power-laws as function of solid volume fraction $\phi$, see insert. The exponents for the shear moduli, $G_i \propto \phi^{\gamma_i}$ with $i = 1, 2$ are found to be close to the literature value 2, and constant as function of $p$. By contrast, the exponent for the bulk modulus $K \propto \phi^{\kappa}$ changes from the expected value $\kappa \approx 1$ at $p = 0$ to $\kappa \approx 2$ for $p \approx 1$.

(vi) In analogy to standard percolation, one may expect the critical behaviour to be independent of the type of underlying network; this expectation should be verified by an analysis of node severing of other four-coordinated networks, such as the crystalline **nbo** network [9] or the network of plateau edges in random isotropic or sheared foams [19, 20].

## Mechanical properties

The remainder of this paper addresses mechanical properties of linear-elastic realizations of the networks with split (or severed) vertices. In porous or cellular structures, the existence of a solid percolating cluster is a prerequisite for mechanical stability, that is, for finite values of the effective linear-elastic moduli. The relationship between percolation critical behaviour and effective elastic properties (those relevant for sample sizes much larger than the micro-structural length scale) is well-known, leading to a power-law decay of the effective elastic moduli near $p_c$ [2, 12]. We employ a voxel-based finite element method [21, 22] to evaluate the effective linear-elastic properties of network solids based on the vertex split model (Some preliminary results, for $p \ll p_c$ far from the percolation critical point, have been published in [10]).

Figure 9 shows that near $p_c$, the effective bulk modulus $K$ (the resistance to hydrostatic compression) is commensurate with a power-law decay, $K \propto |p - p_c|^{f_c}$, with an exponent $f_c \approx 3.0$, significantly different from the known exponent $f_c = 3.75$ [12] for site percolation (An analysis of site percolation with the FEM scheme used yields $f_c = 3.6 \pm 0.1$).

The change in network structure that occurs as $p$ varies from 0 to 1 is reflected in the density dependence of the linear elastic bulk modulus. It is frequently observed that the effective elastic moduli scale as power-laws in the solid volume fraction $\phi$ of the cellular structure; specifically, for the limit $\phi \to 0$ of thin beams, the bulk modulus follows $K \propto \phi^{\kappa}$ with $\kappa = 1$ and the shear moduli $G \propto \phi^{\gamma}$ with $\gamma = 2$ [23]; note that structures with

cubic symmetry, such as the crystallographic diamond network, have three independent elastic moduli, the bulk modulus $K$ and two shear moduli $G_1$ and $G_2$. For the vertex split model, figure 10 shows that the effective exponent $\kappa$ of the bulk modulus varies from a value near 1 (as expected) at $p = 0$ to a value close to 2 when all nodes are disconnected at $p = 1$. The exponents of the shear moduli remain close to the expected value of 2.

This behaviour is somewhat rationalized by the observation that, in ordered cellular structures in the thin beam limit, linear behaviour of elastic moduli is associated with strut compression being the dominant deformation mode, whereas quadratic behaviour is associated with strut bending or torsion [24–26]. The network solids corresponding to the vertex split model appear to undergo a transition from being compression-dominated when fully four-coordinated at $p = 0$ to being bending-dominated in the terminal state (at $p = 1$) which corresponds to a dense set of self-avoiding polymers.

In conclusion, we have demonstrated that randomly severing the four-coordinated vertices of a diamond network leads to a transition, manifest in the fraction of clusters that are percolating. The transition, which is reminiscent of a percolation transition yet with substantially different behaviour to conventional bond/site percolation, occurs at $p_c = 1$ when *all* nodes have been split. While the analysis of this paper has clearly demonstrated that the transition does not follow the critical behaviour of standard bond/site percolation, more research is needed to gain a complete understanding of the critical behaviour of this model.

## Acknowledgments

We thank Andrew Kraynik for advise on mechanical properties of cellular structures, and Günter Last, Sebastian Ziesche and Reimer Kühn for insightful discussion of percolation transitions. We acknowledge the support of the German Science Foundation (DFG) through the Cluster of Excellence 'Engineering of Advanced Materials' and through the research group 'Physics and Geometry of Random Spatial Structure' under grant ME1361/12. We are grateful to the anonymous reviewer for constructive comments and for picking up an inconsistency in our previous determination of $\tau$.

## References

[1] Stauffer D and Aharony A 1994 *Introduction to Percolation Theory* 2nd revised edn (London: Taylor and Francis)
[2] Sahimi M 1994 *Applications of Percolation Theory* 1st edn (London: Taylor & Francis)
[3] Hinrichsen H 2000 Non-equilibrium critical phenomena and phase transitions into absorbing states *Adv. Phys.* **49** 815–958
[4] Ódor G 2004 Universality classes in nonequilibrium lattice systems *Rev. Mod. Phys.* **76** 663–724
[5] Melchert O and Hartmann A K 2008 Negative-weight percolation *New J. Phys.* **10** 043039
[6] Achlioptas D, D'Souza R M and Spencer J 2009 Explosive percolation in random networks *Science* **323** 1453–5
[7] Ziff R M 2009 Explosive growth in biased dynamic percolation on two-dimensional regular lattice networks *Phys. Rev. Lett.* **103** 045701
[8] Grassberger P, Christensen C, Bizhani G, Son S-W and Paczuski M 2011 Explosive percolation is continuous, but with unusual finite size behaviour *Phys. Rev. Lett.* **106** 225701
[9] Delgado-Friedrichs O, O'Keeffe M and Yaghi O M 2003 Three-periodic nets and tilings: regular and quasiregular nets *Acta Cryst.* **A59** 22–7
[10] Nachtrab S, Kapfer S C, Rietzel D, Drummer D, Madadi M, Arns C H, Kraynik A M, Schröder-Turk G E and Mecke K 2012 Tuning elasticity of open-cell solid foams and bone scaffolds via randomized vertex connectivity *Adv. Eng. Mater.* **14** 120–4
[11] Christensen K and Moloney N R 2005 *Complexity and Criticality* (London: Imperial College Press)
[12] Torquato S 2002 *Random Heterogeneous Materials* (Heidelberg: Springer)
[13] van der Marck S C 1998 Calculation of percolation thresholds in high dimensions for fcc, bcc and diamond lattices *Int. J. Mod. Phys.* C **9** 529–40
[14] Nachtrab S 2011 Percolation and elasticity of networks *PhD Thesis* Friedrich-Alexander Universität Erlangen-Nürnberg, Germany
[15] Ziff R M 1986 Test of scaling exponents for percolation-cluster perimeters *Phys. Rev. Lett.* **56** 545–8
[16] Duplantier B and Saleur H 1987 Exact tricritical exponents for polymers at the FTHETA point in two-dimensions *Phys. Rev. Lett.* **59** 539–42
[17] Roux S, Guyon E and Sornette D 1988 Hull percolation *J. Phys. A: Math. Gen.* **21** L475
[18] Aizenman M, Duplantier B and Aharony A 1999 Path-crossing exponents and the external perimeter in 2d percolation *Phys. Rev. Lett.* **83** 1359–62
[19] Kraynik A M, Reinelt D A and van Swol F 2004 Structure of random foam *Phys. Rev. Lett.* **93** 208301
[20] Evans M E, Kraynik A M, Reinelt D A, Mecke K and Schröder-Turk G E 2013 Network like propagation of cell-level stress in sheared random foams *Phys. Rev. Lett.* **111** 138301
[21] Nachtrab S, Kapfer S C, Arns C H, Madadi M, Mecke K and Schröder-Turk G E 2011 Morphology and linear-elastic moduli of random network solids *Adv. Mater.* **23** 2633–7
[22] Kapfer S C, Hyde S T, Mecke K, Arns C H and Schröder-Turk G E 2011 Minimal surface scaffold designs for tissue engineering *Biomaterials* **32** 6875–82
[23] Gibson L J and Ashby M F 1982 The mechanics of three-dimensional cellular materials *Proc. R. Soc.* A **382** 43–59
[24] Warren W E and Kraynik A M 1988 The linear elastic properties of open-cell foams *J. Appl. Mech.* **55** 341–6
[25] Warren W E and Kraynik A M 1997 Linear elastic behaviour of low-density Kelvin foam with open cells *J. Appl. Mech.* **64** 787–94
[26] Christensen R M 2000 Mechanics of cellular and other low-density materials *Int. J. Solids Struct.* **37** 93–104